Письма в ЭЧАЯ. 2013. Т. 10, № 3(180). С. 430–436

ФИЗИКА ТВЕРДОГО ТЕЛА И КОНДЕНСИРОВАННЫХ СРЕД

DETERMINATION OF IVC BREAKPOINT FOR JOSEPHSON JUNCTION STACK. PERIODIC AND NONPERIODIC (WITH $\gamma = 0$) BOUNDARY CONDITIONS

S. I. Serdyukova [1]

Joint Institute for Nuclear Research, Dubna

We prove that in the case of periodic and nonperiodic (with $\gamma = 0$) boundary conditions, the calculation of the current-voltage characteristic for a stack of n intrinsic Josephson junctions reduces to solving a unique equation. The current-voltage characteristic $V(I)$ has the shape of a hysteresis loop. On the back branch of the loop, $V(I)$ rapidly decreases to zero near the breakpoint I_b. We succeeded to derive an equation determining the approximate breakpoint location.

Доказано, что в случае периодических и непериодических (с $\gamma = 0$) граничных условий вычисление вольт-амперной характеристики для системы n внутренних джозефсоновских переходов сводится к решению одного уравнения. Вольт-амперная характеристика $V(I)$ имеет вид петли гистерезиса. На обратной ветви петли гистерезиса значение $V(I)$ быстро спадает к нулю в окрестности критической точки I_b. Нам удалось вывести уравнение, определяющее приближенное значение I_b.

PACS: 60.64

INTRODUCTION

A detailed investigation of the breakpoint current I_b and the breakpoint region width gives important information concerning the occurrence of longitudinal plasma waves and the peculiarities of stacks with a finite number of intrinsic Josephson junctions [1–3]. The breakpoint region in the current-voltage characteristics (IVC) follows from the solution of the system of n dynamical equations of the phase differences for a stack of n intrinsic Josephson junctions. In this work, we prove that in the case of periodic and nonperiodic (with $\gamma = 0$) boundary conditions, the IVC calculation for a stack of n intrinsic Josephson junctions reduces to solving a single equation of the form

$$\ddot{\eta}(t) = -\beta\dot{\eta}(t) + I - \sin(\eta(t)).$$

Solving this equation on the interval $[0, T_{\max}]$ for different I, we get the current-voltage characteristic $V(I)$ as a hysteresis loop. First, the Cauchy problem with the zero initial

[1] E-mail: sis@jinr.ru

conditions, $\eta(I_0, 0) = 0$ and $\dot{\eta}(I_0, 0) = 0$, is solved. For each subsequent $I = I_{k+1}$, the found $\eta(I_k, T_{\max})$ and $\dot{\eta}(I_k, T_{\max})$ are used as initial data. On the back branch of the hysteresis loop, $V(I)$ rapidly decreases to zero near the breakpoint I_b [3]. Effective numerical and analytical methods for IVC calculation were developed in [4]. We succeeded to derive an equation determining the approximate breakpoint location $\tilde{I}_b$. This solves the problem of choosing a point of going from analytical calculations to numerical ones: $I = 2\tilde{I}_b$. This mixed method showed excellent results in IVC calculation for a stack of 9 intrinsic Josephson junctions. The calculations were performed by using the REDUCE 3.8 system.

1. THE HYSTERESIS CALCULATION PROBLEM

The solution of the system

$$\ddot{\phi}_l = \sum_{l'=1}^{n} A_{l,l'}(I - \sin(\phi_{l'}) - \beta\dot{\phi}_{l'}), \quad l = 1, \ldots, n \tag{1}$$

for different $I\,(I = I_0 + k\Delta I \leqslant I_{\max}; I = I_{\max} - k\Delta I)$ yields the current-voltage characteristics of stacks as hysteresis loops [3]. For the initial value of the current, $I = I_0$, the system (1) is solved with zero initial data on the interval $[0, T_{\max}]$. For each subsequent $I\,(I = I_{k+1})$, the found $\phi_l(I_k, T_{\max}), \dot{\phi}_l(I_k, T_{\max})$ are used as initial data.

In the case of periodic boundary conditions, the matrix A is a square matrix of order n

$$\begin{pmatrix} A = 1+2\alpha & -\alpha & 0 & \ldots & 0 & -\alpha \\ -\alpha & 1+2\alpha & -\alpha & 0 & \ldots & 0 \\ 0 & -\alpha & 1+2\alpha & -\alpha & 0 & \ldots \\ \ldots & \ldots & \ldots & \ldots & \ldots & \ldots \\ 0 & \ldots & 0 & -\alpha & 1+2\alpha & -\alpha \\ -\alpha & 0 & \ldots & 0 & -\alpha & 1+2\alpha \end{pmatrix}. \tag{2}$$

Henceforth, the parameter α gives the coupling between junctions, β is the dissipation parameter, and I is the external current normalized to the critical current I_c.

In the case of nonperiodic boundary conditions with $\gamma = 0$, the matrix A is three-diagonal,

$$\begin{pmatrix} A = 1+\alpha & -\alpha & 0 & \ldots & 0 & 0 \\ -\alpha & 1+2\alpha & -\alpha & 0 & \ldots & 0 \\ 0 & -\alpha & 1+2\alpha & -\alpha & 0 & \ldots \\ \ldots & \ldots & \ldots & \ldots & \ldots & \ldots \\ 0 & \ldots & 0 & -\alpha & 1+2\alpha & -\alpha \\ 0 & 0 & \ldots & 0 & -\alpha & 1+\alpha \end{pmatrix}. \tag{3}$$

In the general case of nonperiodic boundary conditions, $a_{1,1} = a_{n,n} = 1 + \alpha(1 + \gamma)$, where $\gamma = s/s_0 = s/s_n$, with s, s_0, s_n denoting the thickness of the middle, first and last superconducting layers, respectively [3]. The condition $\gamma = 0$ simulates the limiting case of negligible thick inner layers, as compared to the two enter layers.

The dynamics of the phases $\phi_l(t)$ has been simulated by solving the system (1) using the fourth-order Runge–Kutta method [5]. After simulation of the phase dynamics, the voltages on each junction were calculated as

$$\frac{\partial \phi_l}{\partial t} = \sum_{l'=1}^{n} A_{l,l'} V_{l'}. \tag{4}$$

The average voltage $\bar{V}_l$ across the lth junction is given by

$$\bar{V}_l = \frac{1}{T_{\max} - T_{\min}} \int_{T_{\min}}^{T_{\max}} V_l \, dt. \tag{5}$$

Finally, the total voltage V of the stack is obtained by summing up these averages:

$$V = \sum_{l=1}^{n} \bar{V}_l. \tag{6}$$

2. THE SYSTEM TRANSFORMATION

The calculation can be simplified using specific properties of the matrices (2) and (3). These matrices are symmetric. They admit complete systems of orthonormal eigenvectors E_l, with real eigenvalues λ_l [6].

The fundamental matrices D, the columns of which are E_l, reduce the A-matrices to diagonal forms:

$$D^* A D = \Lambda = \mathrm{diag}\,(\lambda_1, \lambda_2, \ldots, \lambda_n).$$

After the change of variables

$$\phi_l = \sum_{l'=1}^{n} d_{l,l'} \psi_{l'} \quad \text{and} \quad V_l = \sum_{l'=1}^{n} d_{l,l'} W_{l'},$$

we get the system

$$\ddot{\psi}_l = -\lambda_l \beta \dot{\psi}_l + \lambda_l \cdot I \cdot S_l - \lambda_l \sum_{l'=1}^{n} d_{l',l} \sin(\phi_{l'}), \quad l = 1, \ldots, n,$$

where S_l is the sum of the E_l elements,

$$S_l = \sum_{l'=1}^{n} d_{l',l}.$$

Equations (4) and (5) result in

$$\frac{\partial \psi_l}{\partial t} = \lambda_l W_l, \quad \bar{W}_l = \frac{\psi_l(T_{\max}) - \psi_l(T_{\min})}{\lambda_l (T_{\max} - T_{\min})},$$

respectively, while the total voltage of the stack is given by

$$V = \sum_{l=1}^{n} S_l \cdot \bar{W}_l. \tag{7}$$

3. THE SPECTRAL DATA

In the case of periodic boundary conditions, the eigenvalue problem of A has the solution

$$\lambda_l = 1 + 2\alpha(1 - \cos(\phi_l)), \quad \phi_l = \frac{2\pi(l-1)}{n}, \quad l = 1, \ldots, n;$$

$$E_1 = \frac{1}{\sqrt{n}} \begin{bmatrix} 1 \\ 1 \\ \vdots \\ 1 \end{bmatrix}, \quad E_l = \sqrt{\frac{2}{n}} \begin{bmatrix} \cos(\phi_l) \\ \cos(2\phi_l) \\ \vdots \\ \cos(n\phi_l) \end{bmatrix}, \quad l = 2, \ldots, n;$$

$$S_1 = \sqrt{n}, \quad S_l = 0, \quad l = 2, \ldots, n.$$

Similarly, in the case of nonperiodic boundary conditions with $\gamma = 0$, we get

$$\lambda_l = 1 + 2\alpha(1 - \cos(\phi_l)), \quad \phi_l = \frac{\pi(l-1)}{n}, \quad l = 1, \ldots, n;$$

$$E_1 = \frac{1}{\sqrt{n}} \begin{bmatrix} 1 \\ 1 \\ \vdots \\ 1 \end{bmatrix}, \quad E_l = \sqrt{\frac{2}{n}} \begin{bmatrix} \cos\left(\dfrac{\pi(l-1)}{2n}\right) \\ \cos\left(\dfrac{3\pi(l-1)}{2n}\right) \\ \vdots \\ \cos\left(\dfrac{\pi(2n-1)(l-1)}{2n}\right) \end{bmatrix}, \quad l = 2, \ldots, n;$$

$$S_1 = \sqrt{n}, \quad S_l = 0, \quad l = 2, \ldots, n.$$

Matrices of such kind have been previously noticed as well [7]. The system

$$\ddot{\psi}_1 = -\beta\dot{\psi}_1 + \sqrt{n} \cdot I_0 - \sum_{l'=1}^{n} d_{l',1} \sin(\phi_{l'}),$$

$$\ddot{\psi}_l = -\lambda_l \beta \dot{\psi}_l - \lambda_l \sum_{l'=1}^{n} d_{l',l} \sin(\phi_{l'}), \quad l = 2, \ldots, n,$$

with zero initial conditions, has the solution $\bar{\psi} = [\psi_1^1, 0, \ldots, 0]^*$, where ψ_1^1 is the solution of the equation

$$\ddot{\psi}_1 = -\beta\dot{\psi}_1 + \sqrt{n} \cdot (I_0 - \sin(\psi_1/\sqrt{n})),$$

with zero initial data.

For each subsequent $I, I = I_{k+1}$, solving the system (1) reduces to solving the equation

$$\ddot{\psi}_1 = -\beta\dot{\psi}_1 + \sqrt{n} \cdot (I_{k+1} - \sin(\psi_1/\sqrt{n})),$$

with initial data

$$\psi_1(0) = \psi_1^k(T_{\max}), \quad \dot{\psi}_1(0) = \dot{\psi}_1^k(T_{\max}).$$

We notice that for any $\bar{\psi} = [\psi_1, 0, \ldots, 0]^*$, we have

$$\bar{\phi} = D\bar{\psi} = \psi_1[1, 1, \ldots, 1]^*/\sqrt{n},$$

and, hence,

$$\sum_{l'=1}^{n} d_{l',l} \sin(\phi_{l'}) = S_l \sin(\psi_1/\sqrt{n}),$$

which equals $\sqrt{n}\sin(\psi_1/\sqrt{n})$, when $l = 1$, and zero, when $l = 2, \ldots, n$.

4. ASYMPTOTIC FORMULAS

In both considered cases, the hysteresis calculation problem is reduced to solving the unique equation

$$\ddot{\eta}(t) = -\beta\dot{\eta}(t) + I - \sin(\eta(t)), \tag{8}$$

where $\eta(t) = \psi_1(t)/\sqrt{n}$. Following [8], we replace the search of the solution of (8) with initial data $\eta(0) = d_1$, $\dot{\eta}(0) = d_2$, with the search of the solution of the equivalent integral equation

$$\eta(t) = d_1 + \frac{(d_2 - \omega)}{\beta}(1 - \mathrm{e}^{-\beta t}) + \omega t - \frac{1}{\beta}\int_0^t (1 - \mathrm{e}^{-\beta(t-s)}) \sin(\eta(s))\, ds.$$

Using the simple iterations method

$$\eta_{l+1}(t) = d_1 + \frac{(d_2 - \omega)}{\beta}(1 - \mathrm{e}^{-\beta t}) + \omega t - \frac{1}{\beta}\int_0^t (1 - \mathrm{e}^{-\beta(t-s)}) \sin(\eta_l(s))\, ds, \quad \eta_0 = 0,$$

we get for large t and ω: $\eta_1 = \omega t + A + O(\mathrm{e}^{-\beta t})$,

$$\eta_2(t) = \omega t + A + \theta + \frac{\sin(\omega t + A + \operatorname{arctg}(\beta/\omega))}{\omega\sqrt{\beta^2 + \omega^2}} + O(\omega^{-3} + \mathrm{e}^{-\beta t}), \tag{9}$$

$$\eta_3(t) = \left(\omega - \frac{\cos(\theta)}{2\omega(\omega^2 + \beta^2)} + \frac{\sin(\theta)}{2\beta(\omega^2 + \beta^2)}\right) t + A -$$

$$- \frac{\cos(A + \theta)}{\beta\omega} - \frac{\cos(2A + \theta)}{4\beta\omega^3} - \frac{\sin(\theta - \operatorname{arctg}(\beta/\omega))}{2\beta^2\omega\sqrt{\beta^2 + \omega^2}} +$$

$$+ \frac{\sin(\omega t + A + \theta + \operatorname{arctg}(\beta/\omega))}{\omega\sqrt{\beta^2 + \omega^2}} + O(\omega^{-4} + \mathrm{e}^{-\beta t}). \tag{10}$$

Here $\omega = I/\beta$, $A = d_1 + (d_2 - \omega)/\beta$, $\theta = -\cos(A)/(\omega\beta)$.

Therefore, $V(I, n) = \sqrt{n}\bar{W}_1(I)$ (see (7)),

$$\bar{W}_1(I) = \sqrt{n}\frac{\eta(I, T_{\max}) - \eta(I, T_{\min})}{T_{\max} - T_{\min}}, \text{ and } V(I, n) = n\frac{\eta(I, T_{\max}) - \eta(I, T_{\min})}{T_{\max} - T_{\min}}.$$

5. APPROXIMATE BREAKPOINT LOCATION

The approximate breakpoint location ω can be found from (10) as a solution of the equation $F(\omega) = 0$, where

$$F(\omega) = \omega + \frac{\sin(\theta - \operatorname{arctg}(\beta/\omega))}{2\beta\omega\sqrt{\omega^2+\beta^2}} + \frac{\sin(\omega T_{\max} + A + \theta + \operatorname{arctg}(\beta/\omega))}{\omega\sqrt{\beta^2+\omega^2}(T_{\max} - T_{\min})} - \\ - \frac{\sin(\omega T_{\min} + A + \theta + \operatorname{arctg}(\beta/\omega))}{\omega\sqrt{\beta^2+\omega^2}(T_{\max} - T_{\min})}.$$

Here $A = -\omega/\beta$ for the vanishing initial conditions $d_1 = d_2 = 0$. The polynomial $P(x) = 4\beta^2\omega^4(\omega^2+\beta^2) - 1$ has the unique positive root $xt = 1.35232$. We find that $F(xt) = 1.447\ldots$ and $F(1) = -1.434\ldots$ The approximate breakpoint location is then calculated by using the interval bisection method, $\tilde{I}_b = 0.210248\ldots$ Roughly speaking, the jump to numerical calculations must be done at $2\tilde{I}_b$. In our calculations, we put $T_{\min} = 50$, $T_{\max} = 1000$, $\Delta I = 0.05$. The step in the Runge–Kutta method was $h = 0.1$. All the calculations were performed by using the REDUCE 3.8 system [9].

Figure 1 depicts the back way of the hysteresis loop. The solid and dotted lines refer to numerical and «asymptotic» using (9) calculations, respectively. In Fig. 2, the solid line is the same as in Fig. 1, while the circles on this line refer to calculation performed by the following mixed analytical-numerical method. The right way of the hysteresis loop and the back way on the interval $2\tilde{I}_b < I < 1.45$ are computed using the asymptotic formula (9). The rest points of the hysteresis loop are computed numerically. Figure 3 depicts the back way of the hysteresis loop for $n = 1, 3, 5, 9, 13$, and 17. More precisely, points in these graphs for $n = 3, 5, 9, 13$, and 17 are nothing else, but

$$\left(I_k, n\frac{\eta(I_k, T_{\max}) - \eta(I_k, T_{\min})}{T_{\max} - T_{\min}}\right),$$

where $\eta(I_k, t)$ have been computed by mixing the analytical and numerical approaches.

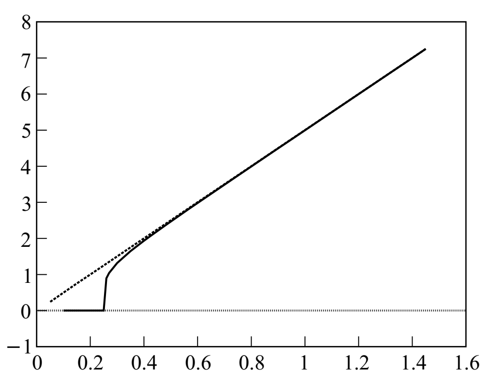

Fig. 1

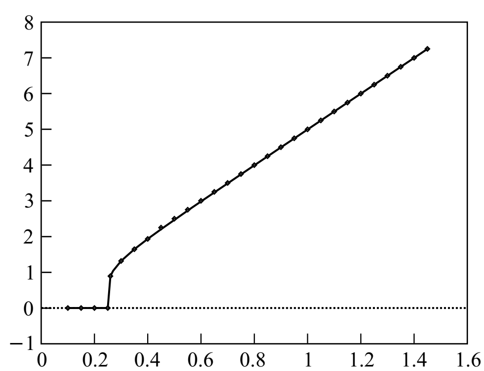

Fig. 2

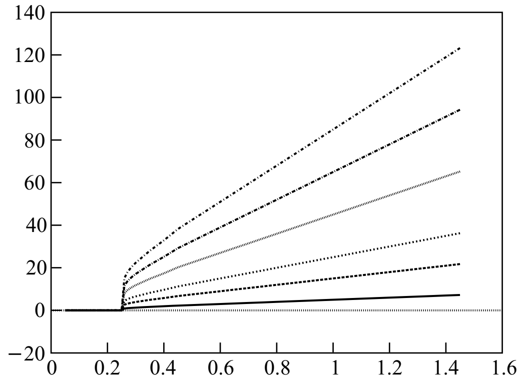

Fig. 3

Acknowledgements. The author is grateful to Yu. M. Shukrinov for the statement of the problem and useful discussions.

REFERENCES

1. *Zappe H. H.* Minimum Current and Related Topics in Josephson Tunnel Junction Devices // J. Appl. Phys. 1973. V. 44, No. 3. P. 1371–1377.
2. *Matsuda Y. et al.* Collective Josephson Plasma Resonance in the Vortex State of $Bi_2Sr_2CaCu_2O_{8+\delta}$ // Phys. Rev. Lett. 1995. V. 75, No. 24. P. 4512–4515.
3. *Shukrinov Yu. M., Mahfousi F., Pedersen N. F.* Investigation of the Breakpoint Region in Stacks with a Finite Number of Intrinsic Josephson Junctions // Phys. Rev. B. 2007. V. 75. P. 104508.
4. *Serdyukova S. I.* Numerical and Analytical Method of the Current-Voltage Characteristics Calculation for Josephson Junction Stacks // Zh. Vychisl. Matematiki i Matem. Fiziki. 2012. V. 52, No. 11.
5. *Bakhvalov N. S.* The Numerical Methods. M.: Nauka, 1973 (in Russian).
6. *Gantmacher F. R.* The Theory of Matrices. N.Y.: Chelsea Publishing Comp., 1959.
7. *Bakhvalov N. S. et al.* Statics and Dynamics of Single-Electron Solitons in Two-Dimensional Arrays of Ultrasmall Tunnel Junctions // Phys. B. 1991. V. 173, No. 3. P. 319–328.
8. *Levinson N.* Asymptotic Behavior of Solutions of Nonlinear Differential Equations // Studies in Appl. Math. 1969. V. XLVIII, No. 4.
9. REDUCE User's Guide for Unix Systems. Version 3.8 by Winfried Neun ZIB. 2004.

Receiced on September 4, 2012.